Acta Cryst. (1959). **12**, 249

The projection topograph: a new method in X-ray diffraction microradiography.

By A. R. Lang,
Division of Engineering and Applied Physics, Harvard University, Cambridge 38, *Massachusetts, U.S.A.*

(*Received* 29 *September* 1958)

Some time ago the author described a method for the examination of crystal sections using penetrating characteristic radiation (Lang, 1957*a*). The 'section topographs' so obtained show imperfections in the interior of the crystal. With this technique it was discovered that individual dislocations can be detected by X-ray diffraction (Lang, 1957*b*, 1958). However, a large number of section topographs must be compared in order to build up a picture of the spatial distribution of imperfections in the crystal. To obtain this information more readily a new method of diffraction microradiography has been developed which shows directly the imperfection distribution in the specimen volume under investigation. Fig. 1

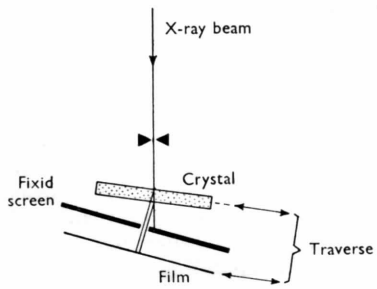

Fig. 1. Plan of the experimental arrangement.

is a plan of the experimental arrangement. The X-ray beam from a relatively distant X-ray tube passes through the specimen crystal after appropriate horizontal and vertical limitation at the slit. The crystal is set so that Bragg reflection occurs from a lattice plane making a high angle with the face of the crystal slab. A fixed screen intercepts the directly transmitted beam but allows the Bragg-reflected beam to reach the film. Crystal and film are both mounted on an accurate linear traversing mechanism. During the exposure they move back and forth together as indicated by arrows. The two-dimensional pattern appearing on the film is a projection of the crystal slab and its imperfection content, hence the name 'projection topograph'. It will be seen that the projection topograph is equivalent to a superimposition of many section topographs. Consequently the maximum imperfection density at which individual imperfections can be resolved is much lower in projection topographs than in section topographs. However, the projection topograph presents a useful survey of the over-all distribution of imperfections. Additional information on the imperfection distribution may be obtained by stereo-diffraction microradiographs composed from a pair of projection topographs, of the hkl and $\bar{h}\bar{k}\bar{l}$ reflections, respectively. Such stereos give a vivid three-dimensional picture of the course of sub-grain boundaries or individual dislocations within the volume of the crystal slab. In the author's apparatus the maximum height of X-ray beam is about $2\frac{1}{2}$ cm. and the maximum length of traverse is also $2\frac{1}{2}$ cm. These dimensions define the maximum area of crystal slab that can be examined in one exposure. In practice, penetrating radiations such as Mo $K\alpha$, Ag $K\alpha$ and W $K\alpha$ have been used so that very thin specimens are not required.

The chief instrumental factor affecting the topographic resolution in the vertical plane is the angular size of the X-ray source. Resolution in the horizontal plane may be affected by the presence of both the $K\alpha_1$ and $K\alpha_2$ images. A typical value for their separation at the film is 10 microns. With good crystals such as silicon it was found convenient to eliminate the $K\alpha_2$ image by reducing the horizontal divergence of the primary beam to about half the difference in Bragg angle of the $K\alpha_1$ and $K\alpha_2$ reflections. The vertical magnification of the image is close to unity. The horizontal magnification is unity if the film is placed parallel to the specimen slab. With thick-emulsion films, however, the film must be kept normal to the diffracted beam. The horizontal magnification is then $\cos(\theta+\alpha)$, in the case when the reflecting plane makes an angle α with the normal to the specimen slab, measured in the same sense as the deviation of the diffracted beam. The horizontal magnification is independent of the direction of crystal traverse, but it is desirable to traverse the specimen slice parallel to its own plane so that the aperture in the fixed screen may be as narrow as possible.

The method has been applied to the study of (i), individual dislocations in nearly perfect crystals, in particular the variation of the strength of the dislocation image with the angle between Buerger's vector and reflecting-plane normal. (A. R. Lang, in preparation); (ii) Pendellösung (N. Kato & A. R. Lang, in preparation); (iii) diffraction effects at sub-grain boundaries (N. Kato & A. R. Lang, in preparation); (iv) precipitates and inclusions in single crystals; (v) new diffraction effects in quartz and calcite; (vi) oxygen bands in silicon;

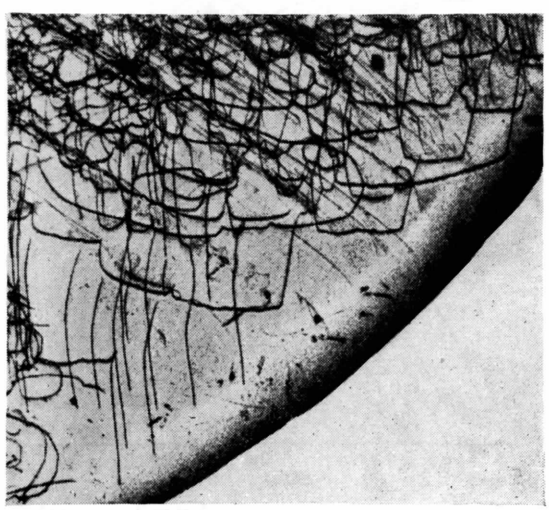

Fig. 2. A projection topograph of dislocations in a {111} slice of silicon, taken with a 220 reflection from planes normal to the slice.

(vii) radiation damage in single crystals; and (viii) influence of the Borrmann effect on diffraction images of dislocations (A. R. Lang, in preparation).

Fig. 2 shows a projection topograph of dislocations in a {111} slice of silicon, taken with a 220 reflection from planes normal to the slice. The area covered is about 5 mm. $\times 4\frac{1}{2}$ mm. Pendellösung fringes may be seen in the bevelled edge of the slice. Noteworthy is the strong visibility of dislocations whose Buerger's vector is normal to the reflecting planes.

This work was made possible by a grant from the National Science Foundation, receipt of which is gratefully acknowledged.

References

LANG, A. R. (1957*a*). *Acta Met.* **5**, 358.
LANG, A. R. (1957*b*). Pittsburgh Diffraction Conference, November, Paper 20.
LANG, A. R. (1958). *J. Appl. Phys.* **29**, 597.

Acta Cryst. (1959). **12**, 250

Determination of lattice parameters directly from Bunn charts.

By P. P. WILLIAMS, *Dominion Laboratory, Wellington, New Zealand*

(*Received* 2 *December* 1958)

Although the Bunn (1945) charts for indexing X-ray powder diffraction patterns of tetragonal and hexagonal structures are easier to use than the Bjurstrom (1931) charts, they suffer from the disadvantage that in plotting values of $1/d^2$ (or $\sin^2\theta$) on a logarithmic scale, knowledge of the actual dimensions of the unit cell is lost, and only the shape of the cell can be deduced directly from the plot. It is often convenient to have a means of checking calculations of axial lengths from indexed lines, and to have the means of deducing rapidly the diffraction pattern that will be produced by a structure with given axial lengths. A simple addition to the Bunn chart allows this to be done.

The Bunn chart is constructed on logarithmic scales, and is used by plotting log $\sin^2\theta$ for lines on the diffraction pattern on a strip of paper, using the same scale as the ordinate of the chart. The strip is moved about on the chart until a good match is obtained between positions of $\sin^2\theta$ and curves on the chart. If in addition to the values of $\sin^2\theta$ for the diffraction maxima, a reference mark at a fixed value of $\sin^2\theta$ is also placed on the strip, information not only about the relative positions of the diffraction lines but also about their actual positions is retained on the strip. At a matching position of the strip, the position on the chart of the reference mark can be correlated with an axial dimension.

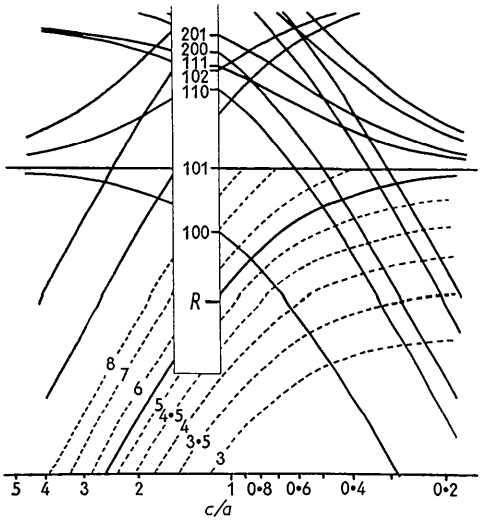

Fig. 1. The Bunn chart for hexagonal structures, with c axial lengths loci marked.
The strip bears the pattern of α-quartz, and a reference mark R, at $\sin^2\theta = 0{\cdot}02$.

At a series of matching positions of the strip, for patterns of structures with one axial length (say the c axis) fixed, and varying axial ratios, the locus of the reference mark is clearly a curve whose vertical distance from the 001 curve on the chart is constant. The distance of the locus from the 001 curve can be calculated, but it is more easily plotted semi-empirically. On a strip of paper is plotted the reference mark to be used, and values of $\sin^2\theta$ corresponding to the 001 spacing for a selection of values of c, at the wavelength to be used. Then the strip is placed vertically on the chart, and the loci of the reference mark plotted as the strip is moved about, keeping each of the $\sin^2\theta$ marks in turn on the 001 curve. Fig. 1 shows the lower part of a Bunn chart for hexagonal structures with the axial-length loci plotted for c axes of 3 Å to 8 Å, for use with a reference mark at $\sin^2\theta = 0{\cdot}02$ and Cu $K\alpha$ radiation. Interpolation between the curves is carried out logarithmically along the ordinate. The strip bears the first few lines of the α-quartz pattern, matched with curves on the chart. The position of the reference mark in relation to the c axial length loci shows the c axis to be 5·43 Å, and the axial ratio, c/a, is read off as usual as 1·10, from which the a axis is calculated as 4·95 Å. Refinement of these axial lengths by considering high-angle lines gives $c = 5{\cdot}405$ Å and $a = 4{\cdot}913$ Å (Swanson & Fuyat, 1953).

The process can be reversed to predict the pattern that a specific structure will produce, by placing a strip of logarithmically calibrated paper on the chart so that the reference-mark position falls at the point on the chart defined by the length of the c axis and the axial ratio. The values of $\sin^2\theta$ at which lines may appear can then be read directly off the strip at the intersections of the edge of the strip with curves on the chart.

References

BJURSTROM, T. (1931). *Z. Phys.* **69**, 346.
BUNN, C. W. (1945). *Chemical Crystallography*. Oxford: Clarendon.
SWANSON, H. E. & FUYAT, R. K. (1953). Nat. Bur. Standards, (U.S.A.) Circ. 539, Vol. III (through the X-ray Powder Data File). Philadelphia, A.S.T.M.